



Preparation of carbon molecular sieve membranes from an optimized ionic liquid-regenerated cellulose precursor

Sandra C. Rodrigues^a, Márcia Andrade^a, Jamie Moffat^b, Fernão D. Magalhães^a, Adélio Mendes^{a,*}

^a LEPABE – Faculdade de Engenharia, Universidade do Porto, Rua Dr. Roberto Frias, 4200-465 Porto, Portugal

^b Innovia Films Ltd., Wigton, Cumbria CA7 9-BG, UK

ARTICLE INFO

Keywords:

Carbon molecular sieve membrane
Water vapor stability
Gas separation
Ionic liquid
Regenerated cellulose

ABSTRACT

Novel carbon molecular sieve membranes with high separation performance and stability in the presence of humidified streams were prepared from an optimized ionic liquid-regenerated cellulose precursor, in a single carbonization step. Membranes prepared at two different carbonization end temperatures (550 °C and 600 °C) were analyzed through scanning electron microscopy, thermogravimetric analysis, Fourier transform infrared spectroscopy, carbon dioxide adsorption and permeation experiments. The prepared membranes exhibited uniform thickness of approximately 20 μm and a well-developed microporous structure. The permeation performance of these carbon molecular sieve membranes was above the Robeson upper bound curve for polymeric membranes. In particular, the membrane prepared at 550 °C end temperature exhibited permeability to oxygen of 5.16 barrer and O₂/N₂ ideal selectivity of 32.3 and permeability to helium of 126 barrer and He/N₂ ideal selectivity of 788; besides, permeation experiments performed in the presence of ca. 80% relative humidity showed that humidity does not originate pore blockage. These results open the door for the preparation of tailor made precursors that originate carbon molecular sieve membranes with extraordinary separation performances, mechanical resistance and stability.

1. Introduction

Over the past few decades, membrane processes for gas separation have improved considerably. Compared to conventional separation techniques, membrane based gas separation is more attractive because of its high adaptability, high reliability, low energy consumption and low capital cost, operation and maintenance, which makes it a more energy-saving and environmental friendly technology [1–4]. On the other hand, carbon molecular sieve membranes (CMSM) have been considered promising candidates for gas separation due to their high corrosion resistance, high thermal stability and excellent permeabilities/permeabilities when compared to polymeric membranes [5–7]. CMSM are prepared from the carbonization of a polymeric precursor under controlled conditions (atmosphere and temperature history); after the carbonization step, CMSM display a highly aromatic structure comprising disordered sp² hybridized carbon sheets packed imperfectly. Pores are formed from packing imperfections between microcrystalline regions in the material [8]; the CMSM structure is turbostratic and described as “slit-like” with a bimodal pore size distribution with micropores connecting ultramicropores [8,9]. Micropores provide sorption sites while ultramicropores (called constrictions)

enable molecular sieving, making CMSM both highly permeable and highly selective - a distinct characteristic of these materials [10–12]. Despite all attractive characteristics displayed by CMSM, they display significant challenges related to their stability when exposed to specific environments [13–15]. In the presence of humidity, water initially adsorbs onto CMSM hydrophilic functional groups and once the first water molecule is adsorbed, adsorbate-adsorbate interactions promote the adsorption of further molecules through hydrogen bonding, originating clusters of several water molecules. The resulting cluster has enough dispersion energy to be released from the hydrophilic group, rolling up until blocking a constriction of the pore network [15]. Consequently, the membrane permeability decreases abruptly, making the carbon membrane useless; this aging effect has seriously limited the commercialization of CMSM.

Up to now, many polymeric precursors have been extensively studied to obtain CMSM with excellent separation performances and stability. These precursors include polyimides [16–20], polyacrylonitrile [21], poly(furfuryl alcohol) [22,23], phenolic resins [24–28], resorcinol-formaldehyde resin [29–32] and cellulose [16,33–35]. Recently, our group applied for a patent of a process for obtaining, in a single carbonization step, CMSM that display no pore blockage effect in

* Corresponding author.

E-mail address: mendes@fe.up.pt (A. Mendes).

<https://doi.org/10.1016/j.memsci.2018.11.027>

Received 22 March 2018; Received in revised form 3 October 2018; Accepted 13 November 2018

Available online 15 November 2018

0376-7388/ © 2018 Elsevier B.V. All rights reserved.

the presence of water vapor and display very high ideal permselectivities for several relevant industrial gas mixtures [36]; these novel carbon molecular sieve membranes were prepared from a commercial cellophane precursor – regenerated cellulose produced by the viscose process. Nevertheless, the obtained CMSM displayed low permeabilities to permanent gases and it was not possible to prepare a tailor made precursor.

Cellulose makes an excellent precursor material for the preparation of CMSM due to its considerable carbon yield, biodegradability, hydrophilicity and low-cost [37–39]. The chemical structure of cellulose consists in anhydroglucose linearly linked by (1,4)- β -D-glucosidic bonds, and the number of molecular glucose units defines its degree of polymerization [37,40]. However, the strong inter and intra hydrogen bonds between cellulose macromolecular chains make it difficult to be dissolved in general solvents [39,41]. The viscose technology uses a metastable solution of cellulose xanthogenate with hazardous by-products like heavy metals and hydrogen sulfide [42–44]; moreover, it generates two kilograms of waste per kilogram of cellulose obtained [45,46]. Other conventional cellulose solvent systems have numerous drawbacks such as limited dissolution capability, toxicity, high cost, uncontrollable side reactions, instability during cellulose processing and/or derivatization [38,47] and negative environmental impacts [48].

Ionic liquids (ILs), a group of salts with poorly coordinated ions and consequently low melting points, represent a promising alternative to existing cellulose-dissolving solvents. ILs have been proposed as environmentally “green solvents”; they present a wide range of melting temperatures (-40–400 °C), have low vapor pressure, excellent dissolution ability, high thermal stability (up to 400 °C), are nonflammable, chemical stability, and ease of recyclability [40,49–51]. ILs are made up of separate cationic and anionic species, but unlike common salts, they have a low tendency to crystallize due to their bulky and asymmetrical cation structure [50]; their properties for a specific need can be tuned combining suitable cations and anions [52]. Moreover, ionic liquids give the opportunity to produce tailor made regenerated cellulose precursor films that allow the preparation of carbon membranes with a high separation performance, mechanical resistance and stability.

In this work, we report the preparation and characterization of regenerated cellulose-based CMSM using an ionic liquid (1-ethyl-3-methyl imidazolium acetate) (EMIMAc) to dissolve cellulose and a spin coating method to cast the precursor membrane. EMIMAc is liquid at room temperature, has high dissolving power even in the presence of 10 wt% of water, relatively low viscosity when compared to other ionic liquids, low toxicity and high hydrogen bond acceptor abilities. Hydrogen bond acceptor sites in the anion structure and lack of hydrogen bond donors in the ionic liquid cation favor the dissolution of cellulose. The acetate anion in 1-ethyl-3-methyl imidazolium acetate can form hydrogen bonds with hydroxyl protons of cellulose (Fig. 1).

To the best of the authors' knowledge, this is the first time that regenerated cellulose films produced through an ionic liquid process are studied for preparation of CMSM. Defect-free CMSM were successfully and reproducibly prepared at two different carbonization end temperatures, 550 °C and 600 °C.

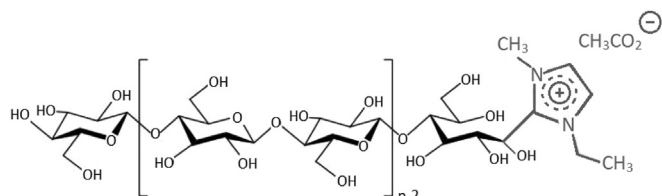


Fig. 1. Schematic representation of cellulose and 1-ethyl-3-methylimidazolium acetate covalent binding (adapted from [42]).

2. Experimental

2.1. Materials

Wood pulp (cellulose) was provided by Innovia Films Ltd., displaying a degree of polymerization (DP) of 450. The ionic liquid 1-ethyl-3-methylimidazolium acetate (EMIMAc) and propylene glycol ($\geq 99.5\%$), used as plasticizer, were supplied by Sigma-Aldrich. Dimethyl sulfoxide (DMSO) was purchased from Fisher Scientific. The permanent gases were supplied by Air Liquid (99.999% pure).

2.2. Preparation of regenerated cellulose precursor membranes

Wood pulp was dispersed in DMSO and EMIMAc (70:30 wt% of DMSO: EMIMAc) to prepare a 9.2 wt% cellulose solution. The mixture was heated at 90 °C under magnetic stirring until cellulose was completely dissolved. After dissolution, the resultant brownish solution was filtered with a wire mesh and placed in a vacuum oven at 40 °C for degassing during 2 h. The obtained homogeneous solution was subsequently spin coated on rectangular glass plates with a spin-coater (POLOS™, SPIN150i) at a spinning speed of 2000 rpm, spin acceleration of 1000 rpm/s and a spinning time of 10 s. After coating, the films were immediately coagulated in distilled water (25 °C) to obtain a transparent regenerated cellulose film. The film was then intensely washed with distilled water for 60 min to remove the excess of ionic liquid. After that, the washed film was dipped in a softener bath containing 5 wt% of propylene glycol for 1 min and then dried in an oven at 100 °C for 10 min Fig. 2 summarizes the preparation steps of the regenerated cellulose precursor membranes.

2.3. Preparation of regenerated cellulose-based carbon molecular sieve membranes

Previous to carbonization, the precursor membranes were cut in disks with 48 mm diameter. The carbonization was then accomplished in a quartz tube (80 mm in diameter and 1.5 m in length) inside a tubular horizontal Termolab TH furnace. To guarantee temperature homogeneity along the quartz tube, the furnace has three separating heating elements controlled by three PID control heating parameters. Fig. 3 gives a schematic overview of the setup for carbonization.

The carbonization was performed under N_2 atmosphere, with flowrate of 170 ml min^{-1} and a heating rate of 0.5 °C min^{-1} . Fig. 4 shows the heating history used to prepare the carbon molecular sieve membranes from regenerated cellulose films. The temperature history comprehends essentially slow heating rates with several dwells of 30 min to avoid a quick release of residual solvents/volatile matter that could damage the carbon matrix, causing cracks/defects. Two end temperatures were considered, 550 °C (CMSM 550) and 600 °C (CMSM 600); after the end temperature was reached, the system was allowed to cool naturally until room temperature, and the flat carbon molecular sieve membranes were finally removed from the carbonization furnace.

2.4. Scanning electron microscopy

Micrographs of the regenerated cellulose precursor membrane and derived CMSM have been taken by scanning electron microscopy (SEM) using a high resolution scanning electron microscope JEOL JSM 6301F/Oxford INCA Energy 350 with x-ray microanalysis. All the samples were previously sputtered with gold/palladium using a SPI Module Sputter Coater equipment to allow better conductivity for SEM.

2.5. Thermogravimetric analysis

Thermogravimetric analysis (TGA) was carried out in a Netzsch TG 209 F1Iris thermogravimetric balance with a resolution of 0.1 μm . The heating procedure [34] consisted on first rise the temperature from

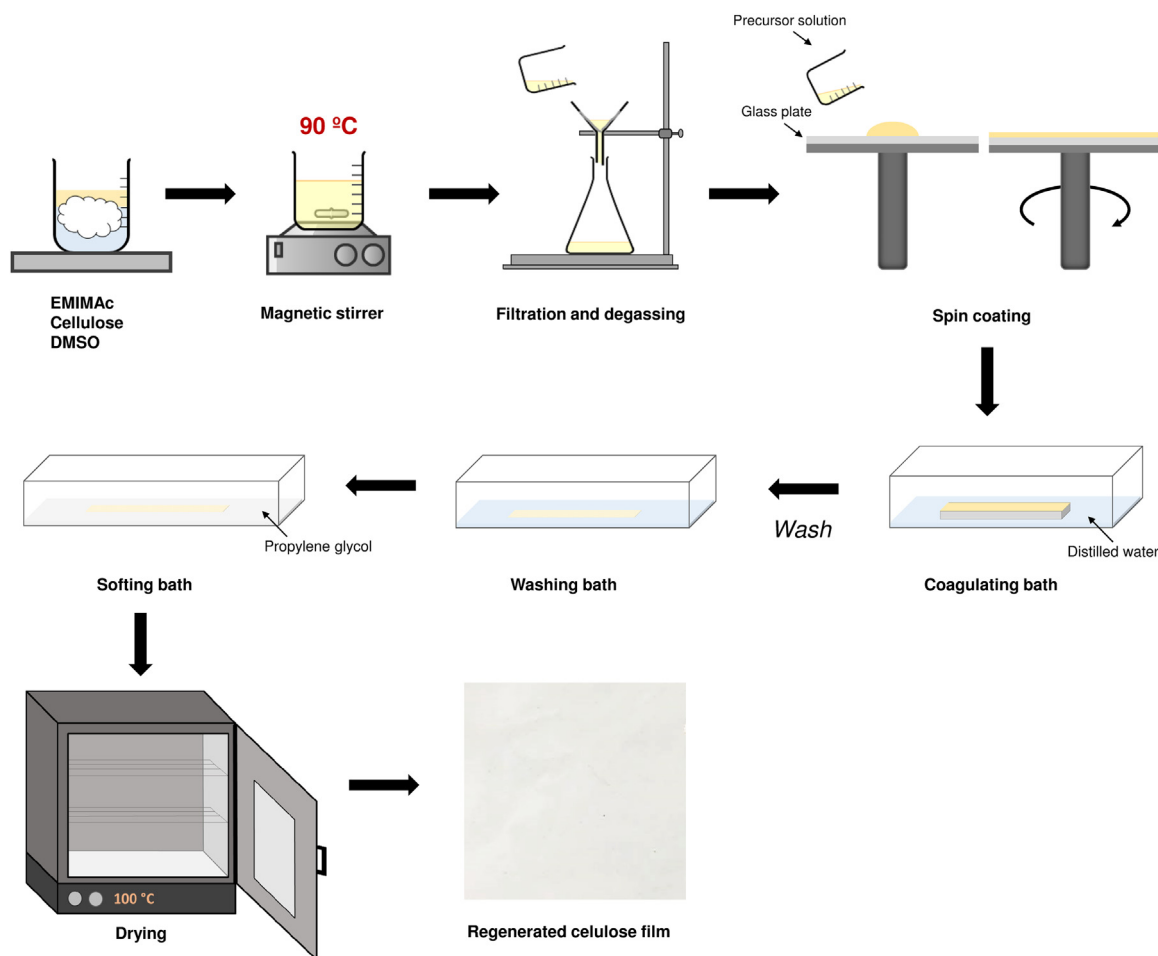


Fig. 2. Preparation steps of the regenerated cellulose precursor membranes.

room temperature to 110 °C at 10 °C min⁻¹, under nitrogen atmosphere, with two dwells at 50 °C (for 10 min) and 110 °C (for 7 min); subsequently, temperature rise from 110 °C to 950 °C with a dwell at 950 °C (for 9 min) and finally the sample was kept at 950 °C for more 11 min under oxygen atmosphere. Proximate analysis was performed to determine the percentage of moisture, volatile matter, carbon yield and ashes content of the precursor material [53]: after the first dwell at 110 °C, humidity is removed; up to the second dwell, volatile matter is released and after the last dwell at 950 °C (under oxygen), all the fixed carbon is burned, leaving only ashes (if present).

2.6. Fourier transform infrared spectroscopy (FTIR)

The infrared spectra of the precursor and derived CMSM were recorded using a VERTEX 70 FTIR spectrometer (BRUKER) in transmittance mode with a high sensitivity DLaTGS detector at room temperature. Samples were measured in ATR mode, with a A225/Q PLATINUM

ATR Diamond crystal with single reflection accessory. The spectra were recorded from 4000 to 500 cm⁻¹ with a resolution of 4 cm⁻¹.

2.7. Pore size distribution

The pore size distribution (PSD) of the CMSM was obtained based on the adsorption equilibrium isotherm of carbon dioxide at 0 °C obtained by the volumetric method. This method is based on pressure variation of the gas after an expansion; assuming for the system an ideal gas behavior and knowing the pressure decrease, the concentration of the adsorbed solute can be determined [54,55]. The apparatus used to perform these experiments is described elsewhere [55].

2.8. Permeation experiments

Prior to permeation experiments, the CMSM were glued to steel O-rings with an epoxy glue (Araldite® Standard); the glue was also applied

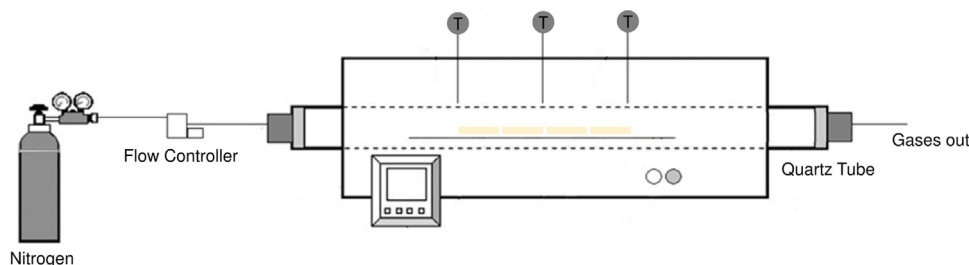


Fig. 3. Carbonization setup used to prepare the regenerated cellulose-based CMSM.

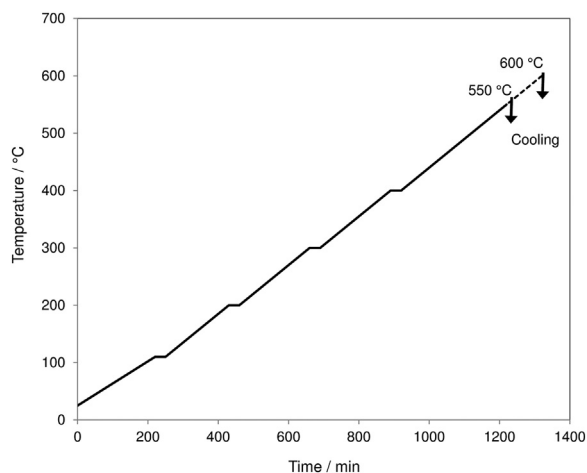


Fig. 4. Carbonization protocol to prepare the regenerated cellulose-based CMSM.

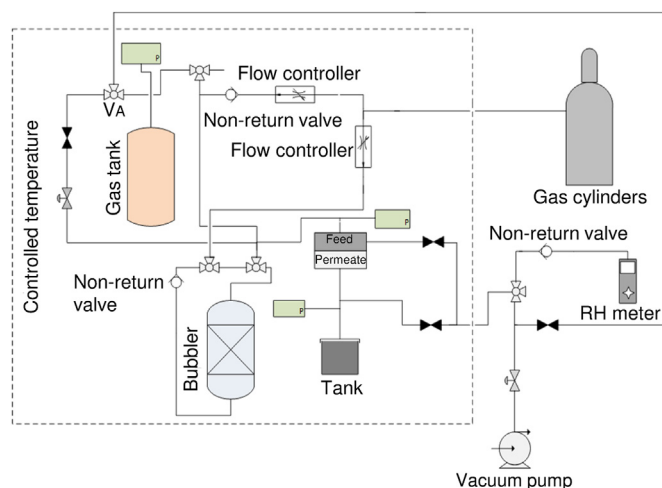


Fig. 5. Scheme of the experimental setup for gas permeation experiments.

along the interface of the steel O-ring and the carbon membrane, as described elsewhere [34]. A sintered metal disc covered with a filter paper was used as support for the film in the test cell. Single gases were tested at 25 °C, where the feed pressure was 1 bar and the permeate pressure was ca. 0.03 bar. The tests were performed in a standard pressure-rise setup with LabView® data logging. As shown in Fig. 5, the system included the membrane cell connected to a tank with a calibrated volume (at the permeate side) and to a gas tank (at the feed side). The feed gas can either be used dry or humidified; for experiments with an humidified gas stream, part of the gas stream from the cylinder was bubbled in a distilled water bubbler, balanced with dry gas for producing the desired humidity level, and fed to the membrane cell. The relative humidity was checked for every run with a RH meter (Vaisala DMP74b) at an exit port.

The permeability of the CMSM towards a pure component i , L_i , was

determined accordingly to:

$$L_i = \frac{F_i}{\Delta P_i / \delta} \quad (1)$$

where F_i is the flux of species i , ΔP_i the partial pressure difference of species i between the two sides of the membrane and δ the membrane thickness (determined by scanning electron microscopy). The membrane permeability to pure component i was computed from the experimental data as follows:

$$L_i = \frac{\delta V_p v_M \Delta P_p}{R T t A (P_f - P_p)} \quad (2)$$

where V_p is the volume of the permeate tank, v_M is the molar volume of the gas at normal conditions, R is the gas constant, T is the absolute temperature, t is the time, A is the effective area of the flat carbon membrane and P_f and P_p are the feed pressure and permeate pressure, respectively; ΔP_p is the permeate pressure increment for the time t . Barrer is the most frequently used unit to express permeability, where 1 barrer = $3.39 \times 10^{-16} \text{ mol m m}^{-2} \text{ s}^{-1} \text{ Pa}^{-1}$. The ratio of two gases permeability coefficients is the ideal selectivity [56]:

$$\alpha_{i,j} = \frac{L_i}{L_j} \quad (3)$$

3. Results and discussion

3.1. Preparation of regenerated cellulose-based CMSM

The prepared regenerated cellulose-based CMSM are identified in Table 1. The precursor disks shrank during the carbonization step and the shrinkage fraction (SH) of each CMSM was determined as follows:

$$SH = \frac{D_{\text{before}} - D_{\text{after}}}{D_{\text{before}}} \times 100 \quad (4)$$

where D_{before} is the membrane diameter before carbonization and D_{after} is the membrane diameter after the carbonization step.

From Table 1, it can be observed that shrinkage increased with the carbonization end temperature. Similarly, the increase in the carbonization end temperature led to a decrease in the membrane thickness (δ , measured by SEM). Fig. 6 shows a membrane before and after carbonization.

3.2. Scanning electron microscopy

The structure of the membranes was examined by SEM. In a previous study, the research team prepared CMSM from commercial cellophane paper (a regenerated cellulose film produced by the viscose process) [36,57]. For the first time carbon molecular sieve membranes with stability to water vapor and oxygen were prepared. However, these cellophane-based CMSM displayed rather low permeabilities. Moreover, the viscose technology uses a metastable solution of cellulose xanthogenate with hazardous byproducts and viscose precursor solution degrades over a period of ca. 3 days; consequently, it is very difficult to produce tailor made membrane precursors. The preparation of cellulosic solutions using the ionic liquid process gives the opportunity for preparing tailor made precursors that originate stable carbon

Table 1
Identification of carbon membranes derived from regenerated cellulose.

Sample	Before carbonization		Carbonization temperature (°C)	After carbonization			Physical properties
	D (mm)	δ (μm)		D (mm)	SH (%)	δ (μm)	
Precursor	48	35.6	–	–	–	–	Transparent, flexible
CMSM 550	48	35.6	550	33	31	20.1	Black, bright, brittle
CMSM 600	48	35.6	600	28	42	18.0	Black, bright, brittle

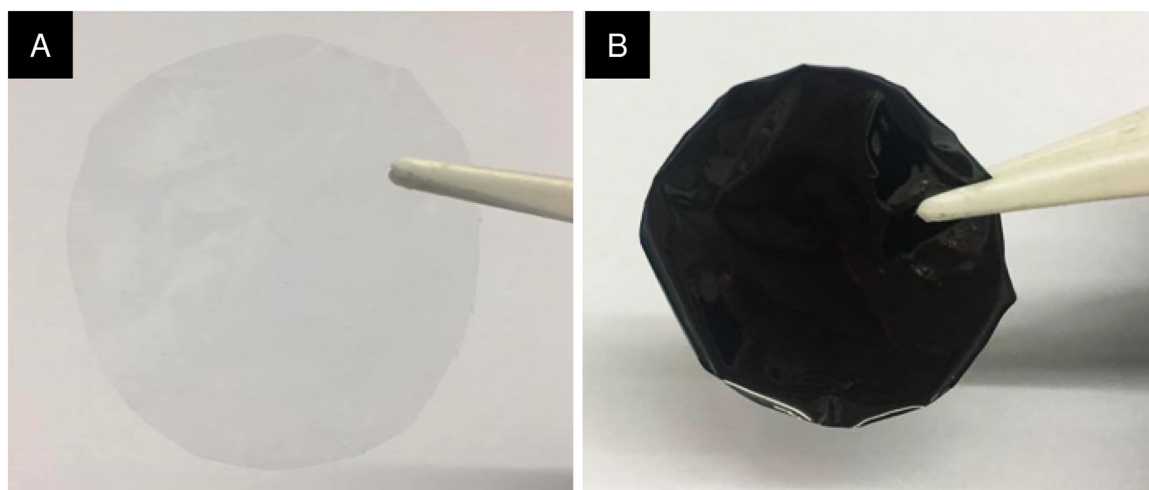


Fig. 6. Regenerated cellulose membrane before (A) and after (B) carbonization.

molecular sieve membranes with adjustable properties depending on the final application.

Fig. 7 shows scanning electron micrographs of surface and cross-sectional views of a CMSM prepared in this work and a cellophane-

based CMSM, both carbonized at 550 °C.

The surface of the sample prepared in this work is very smooth, with no apparent defects (Fig. 7-A) indicating that spin coating is an effective technique for casting the precursor membrane. Microspheres (also

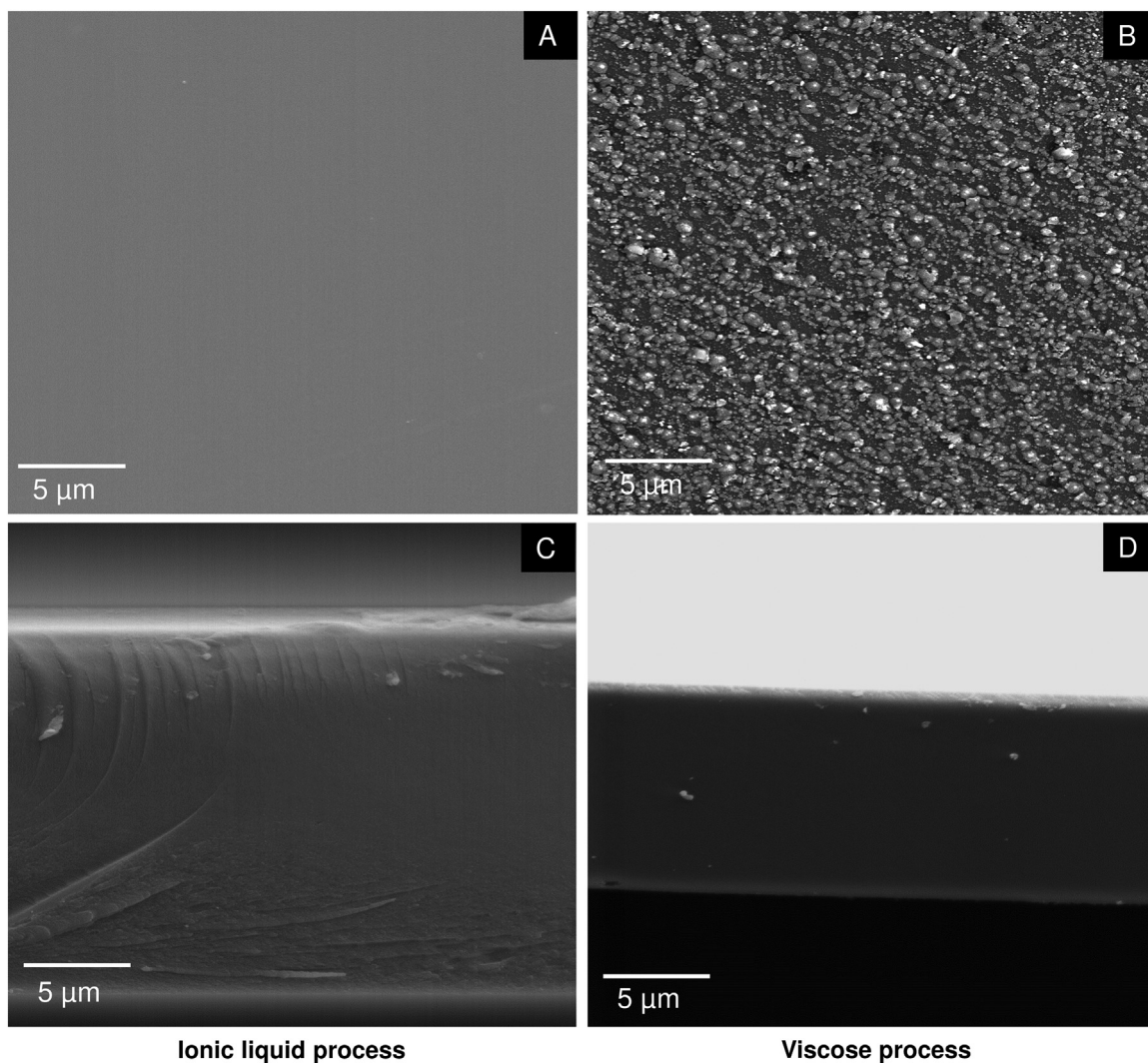


Fig. 7. (A), (B) Surface SEM and (C), (D) cross-sectional images of CMSM obtained from regenerated cellulose films prepared through two different processes: ionic liquid and viscose. Magnification: × 5000. Carbonization end temperature: 550 °C.

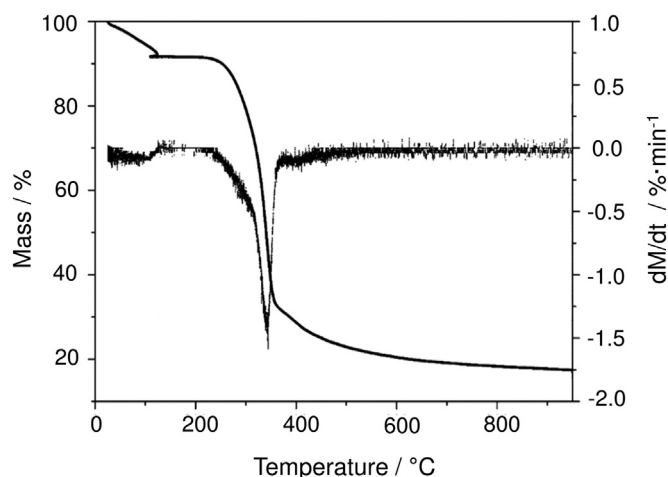


Fig. 8. Thermogravimetric plot and correspondent derivative curve of the regenerated cellulose precursor.

called “condensed benzene rings”) [36,58] were observed on the surface of cellophane-based CMSM (Fig. 7-B) [57] but they were not observed on the surface of CMSM prepared through the ionic liquid process (Fig. 7-A).

3.3. Thermogravimetric analysis

Thermogravimetric analysis was used to assess the thermal decomposition kinetics and stability of precursor in inert atmosphere. TGA was performed on the dry regenerated cellulose film used to prepare the CMSM. The characteristic curve was obtained under N_2 atmosphere and is plotted together with the correspondent mass loss derivative curve in Fig. 8. Up to 100 °C, the first derivative of mass loss curve shows a negative peak related with release of humidity present in the sample. The strong peak around 350 °C corresponds to the larger mass loss and indicates the degradation of the polymer [59] - an abrupt weight loss indicates the onset of the pore network formation [60]. A minute weight loss is observed at ca. 415 °C and the mass still decreasing behind this temperature until 950 °C, but at a much slower rate; at 950 °C the total weight loss was approximately 83%. The regenerated cellulose precursor showed a higher weight loss and at lower temperatures when compared to other polymer precursors commonly used in the preparation of CMSM [24,26,29,60].

Proximate analysis was also performed to determine humidity, volatile matter, fixed carbon and ashes content. Table 2 offers a summary of the results obtained. It was concluded that regenerated cellulose precursor is ash free, presenting ca. 75 wt% of volatile matter and ca. 17 wt% of fixed carbon.

3.4. Fourier transform infrared spectroscopy

The chemical structure of the samples was investigated by Fourier transform infrared spectroscopy. Fig. 9 shows FTIR spectra of the precursor film and derived carbon membranes prepared at 550 °C and 600 °C carbonization end temperature. Band assignments for Fig. 9 are summarized in Table 3.

Table 2

Proximate analysis (dry basis) of the regenerated cellulose precursor.

Proximate analysis (wt%)			
Humidity	Volatile matter	Carbon yield	Ashes
8	75	17	0

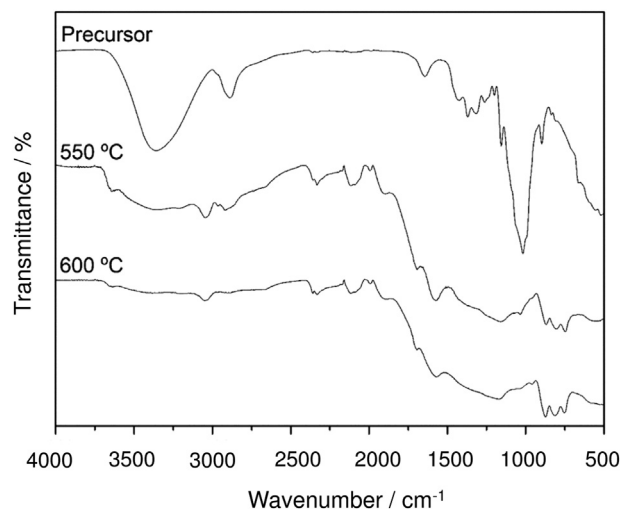


Fig. 9. FTIR spectra of the regenerated cellulose precursor and derived CMSM.

Table 3

FTIR spectra bands assignments.

Wavenumber (cm^{-1})	Functional group	Assignment
3637,3354,3351	-OH	OH stretching
3047	=CH	=C-H stretching
2965,2919,2887	-CH ₃ and -CH ₂ -	Aliphatic C-H stretching
2171	-N≡C	N≡C stretching
1985,1895	Substituted benzene ring	Several bands from overtones and combinations
1693	C=O	C=O stretching
1643	C=C	C=C stretching
1574	COO ⁻	COO ⁻ antisymmetric stretching
1423	CH ₂	CH ₂ bending
1261,1199,1159,1156,897	C-O-C	C-O-C stretching
1034,1018	C-OH	C-O stretching
870,802,746	1,2,4-Trisubstituted benzenes; o-Disubstituted benzenes	Aromatic C-H out-of-plane bending

The precursor spectra show a broad band at 3351 cm^{-1} which is ascribed to the O-H stretching vibrations in hydroxyl or carboxyl groups [61]. The precursor possesses aliphatic structures as it can be deduced from the band at 2887 cm^{-1} , which corresponds to stretching vibrations of aliphatic C-H [61,62]. The band at about 1643 cm^{-1} can be assigned to C=C stretching vibrations and at 1423 cm^{-1} is attributed to CH₂ bending vibrations [63]; the bands at 1261 cm^{-1} , 1199 cm^{-1} and 1156 cm^{-1} correspond at C-O-C antisymmetric stretching vibrations and the peak at 1018 cm^{-1} is assigned to C-O stretching vibrations [64] (C-OH group of secondary alcohols existing in the cellulose chain backbone). The peak detected at 897 cm^{-1} is characteristic of β -(1,4)-glycosidic linkages between glucose units (C-O-C stretching vibrations) [63].

Regarding the CMSM, the spectra of the samples prepared at the two different carbonization end temperatures are similar. However, band intensities are weaker in CMSM obtained at 600 °C than those prepared at 550 °C; this implies that the degree of carbonization in CMSM increases with the carbonization end temperature. Absorption bands at 3637 cm^{-1} and 3354 cm^{-1} , characteristic of O-H stretching vibrations in hydroxyl or carbonyl groups, were observed [61]; at 3047 cm^{-1} a band ascribed to =C-H stretching was also identified [64]. The peaks at 2965 cm^{-1} and 2919 cm^{-1} are related to stretching vibrations of aliphatic C-H (CH₃ and CH₂ groups, respectively) [61,62,64]; however, it was observed that for samples carbonized at 600 °C these two bands disappeared. The band identified at 2171 cm^{-1} , for both samples, is

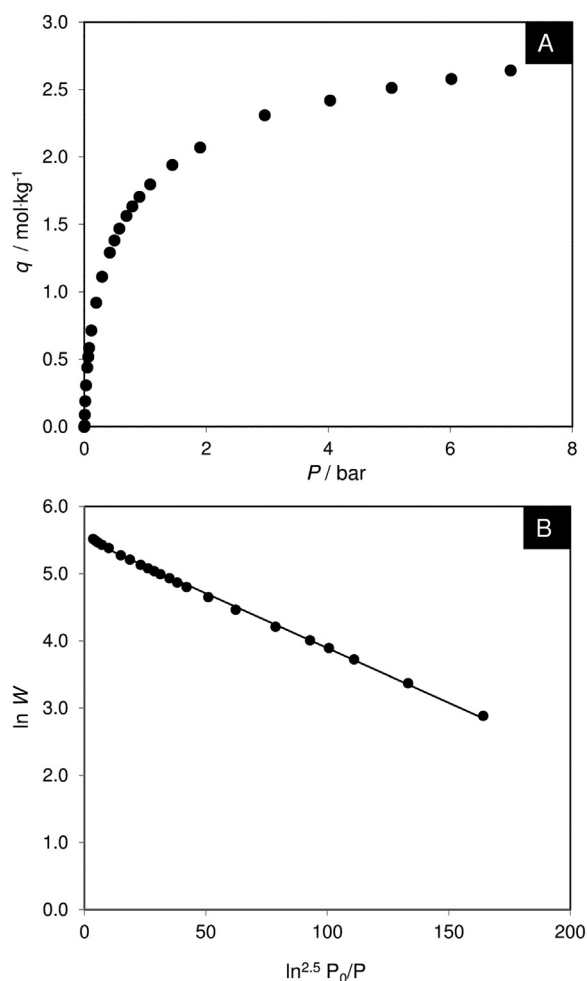


Fig. 10. (A) Adsorption equilibrium isotherm of carbon dioxide at 0 °C and (B) carbon dioxide characteristic curve (points-experimental data; solid line - DA fitting). Carbonization end temperature: 550 °C.

ascribed to $\text{N}=\text{C}$ stretching vibrations [64]; moreover, two bands characteristic of substituted benzene rings were detected at 1995 cm^{-1} and 1895 cm^{-1} [64]. The band at about 1693 cm^{-1} can be assigned to $\text{C}=\text{O}$ stretching vibrations corresponding to carbonyl, quinone, ester or carboxyl [65]; the band at about 1574 cm^{-1} can be assigned to COO^- antisymmetric stretching [64], at 1159 cm^{-1} is attributed to $\text{C}-\text{O}-\text{C}$ antisymmetric stretching vibrations and at 1034 cm^{-1} is assigned to $\text{C}-\text{O}$ stretching vibrations [65]. The bands in the $870\text{--}746 \text{ cm}^{-1}$ region are assigned to aromatic $\text{C}-\text{H}$ out-of-plane bending vibrations [66].

3.5. Pore size distribution

In the present study, the microporosity of the CMSM was assessed based on the adsorption equilibrium isotherm of carbon dioxide at 0 °C; carbon dioxide based pore size distribution is able to describe the CMSM porosity below to the size of CO_2 molecule. Fig. 10 shows the adsorption equilibrium isotherm of carbon dioxide at 0 °C (Fig. 10-A) and the carbon dioxide characteristic curve (Fig. 10-B) for the sample carbonized at 550 °C, as an example. The Dubinin-Astakhov equation was used to fit the experimental data, and to obtain the micropore volume (W_0) and the characteristic energy of adsorption (E_0) [29,67]. Table 4 summarizes the obtained structural parameters for each carbon membrane.

The obtained micropore volume for CMSM 550 is typical for carbon molecular sieves; for CMSM 600, the micropore volume of $327.4 \text{ cm}^3 \text{ kg}^{-1}$ is slightly higher [68,69]. The obtained mean pore widths are

Table 4
Structural parameters.

	Ionic liquid process		Viscose process [57]	
	CMSM 550	CMSM 600	CMSM 550	CMSM 600
$W_0 (\text{cm}^3 \text{ kg}^{-1})$	250.2	327.4	274.2	322.5
$E_0 (\text{kJ mol}^{-1})$	11.79	11.85	12.30	12.71
$l (\text{nm})$	0.711	0.700	0.667	0.635

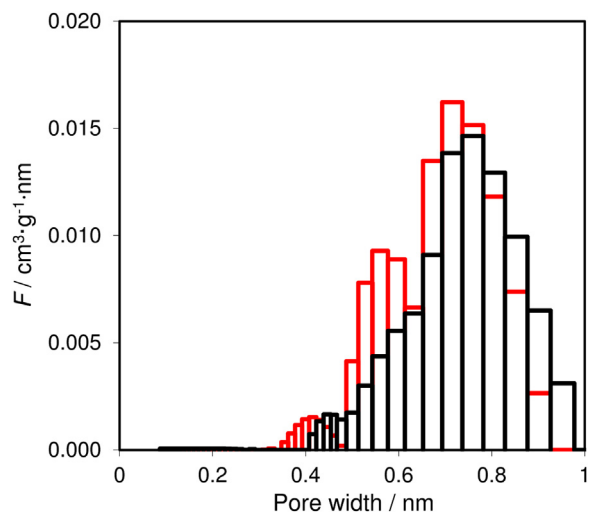


Fig. 11. Micropore size distribution of regenerated cellulose based-CMSM. Ionic liquid process: black line; viscose process: red line. Carbonization end temperature: 550 °C (For interpretation of the references to color in this figure legend, the reader is referred to the web version of this article.).

slightly higher when compared to other reported values [29,68–70]. Comparing the values with the values obtained for cellophane-based CMSM [57] (viscose process), it is possible to observe that these membranes have a higher mean pore width, which is in accordance with the obtained higher permeabilities as will be shown in Section 3.6.

The pore size distribution was obtained using the structure-based method proposed by Nguyen et al. for the determination of the micropore size distribution in carbonaceous materials [71,72]. Fig. 11 and Fig. 12 show the obtained micropore size distributions for CMSM 550

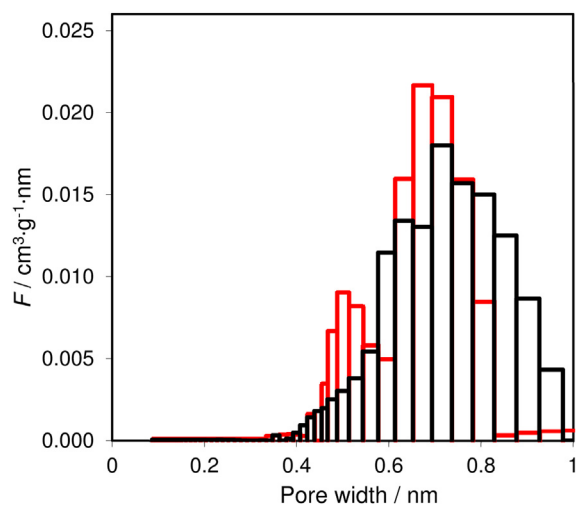


Fig. 12. Micropore size distribution of regenerated cellulose based-CMSM. Ionic liquid process: black line; viscose process: red line. Carbonization end temperature: 600 °C (For interpretation of the references to color in this figure legend, the reader is referred to the web version of this article.).

Table 5
Permeabilities and ideal selectivities for regenerated cellulose-based CSM at 25 °C.

Gas species	CSM 550		CSM 600	
	Permeability (barrer)	Permselectivity X/N ₂	Permeability (barrer)	Permselectivity X/N ₂
N ₂	0.16	–	0.09	–
O ₂	5.16	32.3	2.19	24.3
CO ₂	13.4	83.8	4.18	46.4
He	126	788	174	1993
H ₂	206.0	1288	121	1344

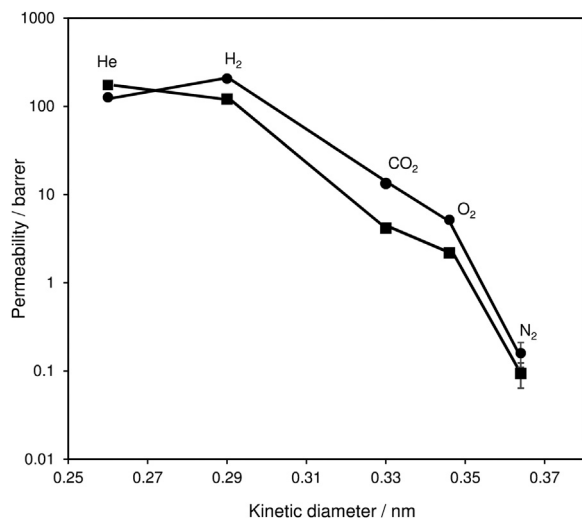


Fig. 13. Permeability as a function of the gas kinetic diameter for regenerated cellulose-based membranes carbonized at • 550 °C and ■ 600 °C, the variance bars of 3 reads were added. Lines were added for readability.

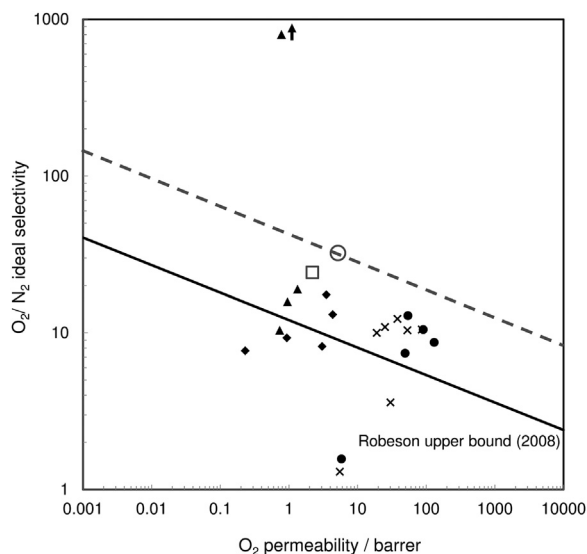


Fig. 14. Gas permeation results for O₂/N₂ in ○ CSM 550, □ CSM 600 and reported cellulose-based CSM (◆ [34]; • [33]; ▲ [36,57]; × [78]) and comparison with the respective upper bound plot.

and CSM 600, respectively, and a comparison with the PSD obtained for cellophane-based CSM [57].

From Figs. 11 and 12, it can be seen that the carbon molecular sieve membranes prepared in this work at two different carbonization end temperatures present ultramicropores (0.4–0.7 nm range) and

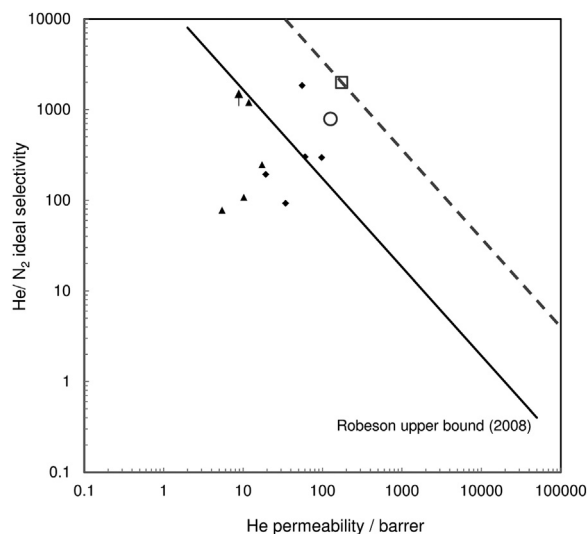


Fig. 15. Gas permeation results for He/N₂ in ○ CSM 550 and □ CSM 600 and reported cellulose-based CSM (◆ [34]; ▲ [36,57]; × [78]) and comparison with the respective upper bound plot.

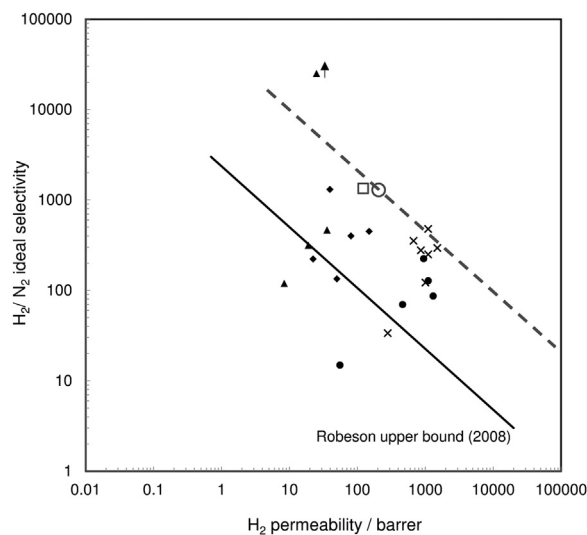


Fig. 16. Gas permeation results for H₂/N₂ in ○ CSM 550 and □ CSM 600 and reported cellulose-based CSM (◆ [34]; • [33]; ▲ [36,57]; × [78]) and comparison with the respective upper bound plot.

micropores (0.7–1 nm). The regenerated cellulose-based CSM (ionic liquid process) prepared at 550 °C and 600 °C present a micropore size distribution slightly shifted to the right, towards higher pore sizes when compared to the cellophane-based; once more, this is in accordance with the obtained higher permeabilities and low ideal selectivities (Section 3.6).

3.6. Permeation experiments

The membranes were tested for permeation using several probe species: nitrogen (0.378 nm), oxygen (0.346 nm), carbon dioxide (0.335 nm), hydrogen (0.290 nm) and helium (0.260 nm) – the values in brackets correspond to the kinetic diameter of the gases [70]. Table 5 presents the obtained permeabilities and ideal selectivities for the regenerated cellulose-based CSM prepared at 550 °C and 600 °C.

Fig. 13 shows the permeability towards several gas species against their kinetic diameter.

Carbon molecular sieve membranes comprise rigid micropore and ultramicropores regions and permeation through these membranes

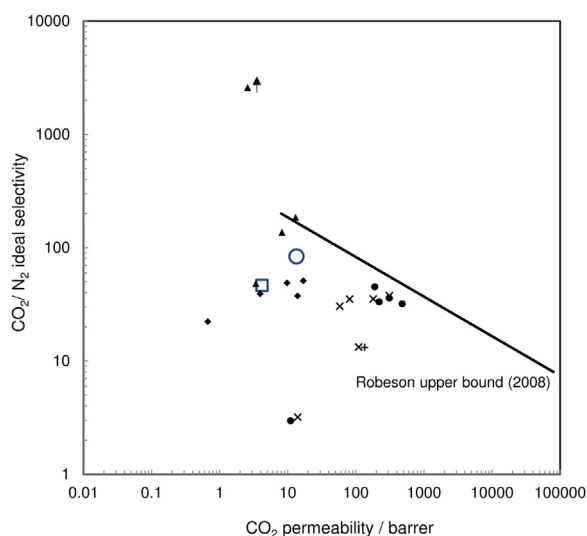


Fig. 17. Gas permeation results for CO_2/N_2 in \circ CMSM 550 and \square CMSM 600 and reported cellulose-based CMSM (\blacklozenge [34]; \bullet [33]; \blacktriangle [36,57]; \times [78]; $+$ [77]) and comparison with the respective upper bound plot.

follows a sorption-diffusion mechanism. The micropores provide sorption sites (gas molecules hop from site to site due to a transmembrane concentration gradient) and ultramicropores provide diffusion restrictions with the ability of discriminate gas molecules based on their size and shape; therefore, ultramicropores control the transport behavior of carbon molecular sieve membranes and determine most of the observed selectivity [73,74]. From Fig. 13, it can be observed that the membrane permeability follows the kinetic diameter of the permeant species. Also, hydrogen with a larger kinetic diameter than helium, permeates faster for CMSM 550 samples; this fact has been reported by other authors [34,75] showing the extent of adsorption (larger for hydrogen than for helium). The effect of carbonization end temperature on the gas performance of regenerated cellulose-based CMSM is also demonstrated in Fig. 13 and Table 5. The samples carbonized at higher temperature (CMSM 600) have generally smaller gas permeation; for example, the membrane permeability towards nitrogen became around 1.8 times smaller when compared to CMSM 550 - rates - CMSM 550 have a larger mean pore width compared to CMSM 600 (Table 4). At 600 °C, carbon atoms are rearranging into a tighter structure, by a sintering mechanism [34,76]. However, CMSM 600 have a larger volume of ultramicropores (Figs. 11 and 12), leading to a higher permeability to helium [29]. However, though this sample displays more pores they are smaller making the permeability of this sample to the other gases smaller than for sample CMSM 550.

The performance of a carbon membrane towards a separation is characterized by the gas permeability as well as the correspondent selectivity. In 2008, Robeson proposed a selectivity/permeability upper bound for representative binary gas separations performed with polymeric membranes. Figs. 14–17 illustrate the Robeson upper bounds for O_2/N_2 (Fig. 14), He/N_2 (Fig. 15), H_2/H_2 (Fig. 16) and CO_2/N_2 (Fig. 17), together with the results obtained in this work; a comparison with CMSM produced from other cellulosic precursors reported in literature [33,34,36,57,77,78] is also included. For facilitating the comparison, a

dashed line was drawn over the best sample of the present work, parallel to the Robeson line. All values below this line perform worse and vice-versa. Robeson upper bounds are broadly recognized as the state-of-the-art curves for gas separation.

It can be observed that the CMSM prepared in this work are plotted above the upper bound for O_2/N_2 , He/N_2 and H_2/N_2 separations. Moreover, when these membranes are compared to the reported cellulosic-based CMSM, (see dashed line) they show a better permeability/permeability balance (except for the cellophane-based CMSM prepared in our previous work) for most of the studied gas separations.

3.6.1. Relative humidity stability

Permeation experiments in the presence of 75–77% RH were undertaken using the regenerated cellulose-based CMSM to determine its performance stability in the presence of water vapor. Table 6 shows the permeability of CMSM 550 and CMSM 600 samples to dry and humidified oxygen and nitrogen. Permeation data showed that humidity does not originate pore blockage for RH above ca. 30–40% as reported for all carbon molecular sieve membranes [13,79]. For carbon membrane samples prepared at 550 °C, the overall permeability increased ca. 1.6 times (the permeability to oxygen stays roughly constant); for carbon membrane samples prepared at 600 °C, the overall permeability increased ca. 2.7 times. This increase is due to the very fast permeation of water vapor that occurs due to the membrane's high hydrophilicity. Previous studies by the authors demonstrated that the high hydrophilicity is characteristic of regenerated cellulose-based CMSM [57].

4. Conclusions

Carbon molecular sieve membranes with high separation performance and stability in the presence of humidity were successfully prepared in a single carbonization step, without need for pre nor post treatments steps. The carbon membranes were prepared from regenerated cellulose, a renewable low cost precursor, using an ionic liquid as cellulose solvent and spin coating for casting the precursor film. Ionic liquids are environmentally friendly and more efficient solvents than current methodologies to dissolve and process cellulose. This was the first time that regenerated cellulose films produced through an ionic liquid process were studied for preparation of CMSM. The permeability versus kinetic diameter towards nitrogen, carbon dioxide, oxygen, hydrogen and helium exhibited a molecular sieve mechanism for the prepared membranes. The effect of carbonization end temperature was assessed, and better separation performances were found for CMSM 550 sample, carbonized in an inert atmosphere at 550 °C. The Robeson upper bound for polymeric membranes was overtaken by the prepared membranes regarding O_2/N_2 , He/N_2 and H_2/N_2 separations.

The produced carbon molecular sieve membranes are stable and have a great potential for gas separation; therefore, they might be considered in relevant industrial applications such as separation of nitrogen from air, air dehumidification and separation of hydrogen from syngas.

Acknowledgments

S.C. Rodrigues is grateful to the Portuguese Foundation for Science and Technology (FCT) for the doctoral grant (reference SFRH/BD/

Table 6
Permeability of CMSM 550 and CMSM 600 to dry and humidified oxygen and nitrogen.

Sample	RH (%)	Dry feed		Humidified feed	
		Permeability to O_2 (barrer)	Permeability to N_2 (barrer)	Permeability to humidified O_2 (barrer)	Permeability to humidified N_2 (barrer)
CMSM 550	75–77	5.16	0.16	8.47	1.33
CMSM 600	75–77	2.19	0.09	5.96	0.85

93779/2013) supported by funding POPH/FSE. M. Andrade is thankful to POCI-01-0145-FEDER-006939 (Laboratory for Process Engineering, Environment, Biotechnology and Energy – UID/EQU/00511/2013) funded by the European Regional Development Fund (ERDF), through COMPETE2020 - Programa Operacional Competitividade e Internacionalização (POCI) and by national funds, through FCT - Fundação para a Ciência e a Tecnologia and NORTE-01-0145-FEDER-000005 – LEPABE-2-ECO-INNOVATION, supported by North Portugal Regional Operational Programme (NORTE 2020), under the Portugal 2020 Partnership Agreement, through the European Regional Development Fund (ERDF) for the fellowship grant. The authors are thankful to Innovia Films Ltd. for generously providing wood pulp.

References

- Q. Liu, T. Wang, H. Guo, C. Liang, S. Liu, Z. Zhang, Y. Cao, D.S. Su, J. Qiu, Controlled synthesis of high performance carbon/zeolite T composite membrane materials for gas separation, *Microporous Mesoporous Mater.* 120 (2009) 460–466.
- X. Ma, B.K. Lin, X. Wei, J. Kniep, Y.S. Lin, Gamma-alumina supported carbon molecular sieve membrane for propylene/propane separation, *Ind. Eng. Chem. Res.* 52 (2013) 4297–4305.
- T.C. Merkel, H. Lin, X. Wei, R. Baker, Power plant post-combustion carbon dioxide capture: an opportunity for membranes, *J. Membr. Sci.* 359 (2010) 126–139.
- R. Faiz, K. Li, Polymeric membranes for light olefin/paraffin separation, *Desalination* 287 (2012) 82–97.
- W. Wei, G. Qin, H. Hu, L. You, G. Chen, Preparation of supported carbon molecular sieve membrane from novolac phenol-formaldehyde resin, *J. Membr. Sci.* 303 (2007) 80–85.
- A.F. Ismail, L.B. David, A review on the latest development of carbon membranes for gas separation, *J. Membr. Sci.* 193 (2001) 1–18.
- P.S. Tin, T.-S. Chung, S. Kawi, M.D. Guiver, Novel approaches to fabricate carbon molecular sieve membranes based on chemical modified and solvent treated polyimides, *Microporous Mesoporous Mater.* 73 (2004) 151–160.
- M. Kiyono, P.J. Williams, W.J. Koros, Effect of pyrolysis atmosphere on separation performance of carbon molecular sieve membranes, *J. Membr. Sci.* 359 (2010) 2–10.
- P.J. Williams, W.J. Koros, Gas separation by carbon membranes, in: N.N. Li, A.G. Fane, W.S.W. Ho, T. Matsuura (Eds.), *Advanced Membrane Technology and Applications*, John Wiley & Sons, New Jersey, 2008, pp. 599–627.
- A.F. Ismail, D. Rana, T. Matsuura, H.C. Foley, Carbon-based Membranes for Separation Processes, first ed., Springer, New York, 2011.
- M.A.L. Tanco, D.A.P. Tanaka, Recent Advances on carbon molecular sieve membranes (CMSMs) and reactors, *Processes* 4 (2016) 1–29.
- A. Mendes, F.D. Magalhães, C.A.V. Costa, New trends on membrane science, in: W.C. Conner, J. Fraissard (Eds.), *Fluid Transport in Nanoporous Materials*, Springer, The Netherlands, 2006, p. 686.
- C.W. Jones, W.J. Koros, Characterization of ultramicroporous carbon membranes with humidified feeds, *Ind. Eng. Chem. Res.* 34 (1995) 158–163.
- I. Menendez, A.B. Fuertes, Aging of carbon membranes under different environments, *Carbon* 39 (2001) 733–740.
- S. Lagorsse, M.C. Campo, F.D. Magalhães, A. Mendes, Water adsorption on carbon molecular sieve membranes: experimental data and isotherm model, *Carbon* 43 (2005) 2769–2779.
- K.M. Steel, W.J. Koros, An investigation of the effects of pyrolysis parameters on gas separation properties of carbon materials, *Carbon* 43 (2005) 1843–1856.
- X. Ma, R. Swaidan, B. Teng, H. Tan, O. Salinas, E. Litwiller, Y. Han, I. Pinnau, Carbon molecular sieve gas separation membranes based on an intrinsically microporous polyimide precursor, *Carbon* 62 (2013) 88–96.
- X. Ning, W.J. Koros, Carbon molecular sieve membranes derived from Matrimid® polyimide for nitrogen/methane separation, *Carbon* 66 (2014) 511–522.
- O. Salinas, X. Ma, E. Litwiller, I. Pinnau, High-performance carbon molecular sieve membranes for ethylene/ethane separation derived from an intrinsically microporous polyimide, *J. Membr. Sci.* 500 (2016) 115–123.
- Y.-J. Fu, C.-C. Hu, D.-W. Lin, H.-A. Tsai, S.-H. Huang, W.-S. Hung, K.-R. Lee, J.-Y. Lai, Adjustable microstructure carbon molecular sieve membranes derived from thermally stable polyetherimide/polyimide blends for gas separation, *Carbon* 113 (2017) 10–17.
- L.B. David, A.F. Ismail, Influence of the thermastabilization process and soak time during pyrolysis process on the polyacrylonitrile carbon membranes for O₂/N₂ separation, *J. Membr. Sci.* 213 (2003) 285–291.
- Y.D. Chen, R.T. Yang, Preparation of carbon molecular sieve membrane and diffusion of binary mixtures in the membrane, *Ind. Eng. Chem. Res.* 33 (1994) 3146–3153.
- C. Song, T. Wang, X. Wang, J. Qiu, Y. Cao, Preparation and gas separation properties of poly(furfuryl alcohol)-based C/CMS composite membranes, *Sep. Purif. Technol.* 58 (2008) 412–418.
- M.A.L. Tanco, D.A.P. Tanaka, S.C. Rodrigues, M. Teixeira, A. Mendes, Composite-alumina-carbon molecular sieve membranes prepared from novolac resin and boehmite. Part I: preparation, characterization and gas permeation studies, *Int. J. Hydrog. Energy* 40 (2015) 5653–5663.
- A.B. Fuertes, I. Menendez, Separation of hydrocarbon gas mixtures using phenolic resin-based carbon membranes, *Sep. Purif. Technol.* 28 (2002) 29–41.
- M. Teixeira, M.C. Campo, D.A.P. Tanaka, M.A.L. Tanco, C. Magen, A. Mendes, Composite phenolic resin-based carbon molecular sieve membranes for gas separation, *Carbon* 49 (2011) 4348–4358.
- W. Zhou, M. Yoshino, H. Kita, K.-i. Okamoto, Carbon molecular sieve membranes derived from phenolic resin with a pendant sulfonic acid group, *Ind. Eng. Chem. Res.* 40 (2001) 4801–4807.
- M. Teixeira, S.C. Rodrigues, M. Campo, D.A. Pacheco Tanaka, M.A. Llosa Tanco, L.M. Madeira, J.M. Sousa, A. Mendes, Boehmite-phenolic resin carbon molecular sieve membranes-permeation and adsorption studies, *Chem. Eng. Res. Des.* 92 (2014) 2668–2680.
- S.C. Rodrigues, R. Whitley, A. Mendes, Preparation and characterization of carbon molecular sieve membranes based on resorcinol-formaldehyde resin, *J. Membr. Sci.* 459 (2014) 207–216.
- M. Yoshimune, T. Yamamoto, M. Nakaiwa, K. Haraya, Preparation of highly mesoporous carbon membranes via a sol-gel process using resorcinol and formaldehyde, *Carbon* 46 (2008) 1031–1036.
- Y.-R. Dong, M. Nakao, N. Nishiyama, Y. Egashira, K. Ueyama, Gas permeation and pervaporation of water/alcohols through the microporous carbon membranes prepared from resorcinol/formaldehyde/quaternary ammonium compounds, *Sep. Purif. Technol.* 73 (2010) 2–7.
- S. Tanaka, T. Yasuda, Y. Katayama, Y. Miyake, Pervaporation dehydration performance of microporous carbon membranes prepared from resorcinol/formaldehyde polymer, *J. Membr. Sci.* 379 (2011) 52–59.
- J.A. Lie, M.-B. Hägg, Carbon membranes from cellulose: synthesis, performance and regeneration, *J. Membr. Sci.* 284 (2006) 79–86.
- M.C. Campo, F.D. Magalhães, A. Mendes, Carbon molecular sieve membranes from cellophane paper, *J. Membr. Sci.* 350 (2010) 180–188.
- M.C. Campo, F.D. Magalhães, A. Mendes, Separation of nitrogen from air by carbon molecular sieve membranes, *J. Membr. Sci.* 350 (2010) 139–147.
- A. Mendes, M. Andrade, M. Boaventura, S.C. Rodrigues, A carbon molecular sieve membrane, method of preparation and uses thereof, Patent WO 2017068517 A1, 2017.
- H. Wang, G. Gurau, R.D. Rogers, Ionic liquid processing of cellulose, *Chem. Soc. Rev.* 41 (2012) 1519–1537.
- J. Pang, X. Liu, X. Zhang, Y. Wu, R. Sun, Fabrication of cellulose film with enhanced mechanical properties in ionic liquid 1-allyl-3-methylimidazolium chloride (AmimCl), *Materials* 6 (2013) 1270.
- B. Ma, A. Qin, X. Li, C. He, Preparation of cellulose hollow fiber membrane from bamboo pulp/1-butyl-3-methylimidazolium chloride/dimethylsulfoxide system, *Ind. Eng. Chem. Res.* 52 (2013) 9417–9421.
- Z.C. Zhang, Catalytic transformation of carbohydrates and lignin in ionic liquids, *WIREs Energy Environ.* 2 (2013) 655–672.
- S. Mahmoudian, M.U. Wahit, A.F. Ismail, A.A. Yussuf, Preparation of regenerated cellulose/montmorillonite nanocomposite films via ionic liquids, *Carbohydr. Polym.* 88 (2012) 1251–1257.
- S. Livazovic, Z. Li, A.R. Behzad, K.V. Peinemann, S.P. Nunes, Cellulose multilayer membranes manufacture with ionic liquid, *J. Membr. Sci.* 490 (2015) 282–293.
- A. Pinkert, K.N. Marsh, S. Pang, M.P. Staiger, Ionic liquids and their interaction with cellulose, *Chem. Rev.* 109 (2009) 6712–6728.
- H.-Z. Chen, N. Wang, L.-Y. Liu, Regenerated cellulose membrane prepared with ionic liquid 1-butyl-3-methylimidazolium chloride as solvent using wheat straw, *J. Chem. Technol. Biotechnol.* 87 (2012) 1634–1640.
- M.T. Clough, K. Geyer, P.A. Hunt, S. Son, U. Vagt, T. Welton, Ionic liquids: not always innocent solvents for cellulose, *Green Chem.* 17 (2015) 231–243.
- B. Kosan, C. Michels, F. Meister, Dissolution and forming of cellulose with ionic liquids, *Cellulose* 15 (2008) 59–66.
- J.-H. Pang, X. Liu, M. Wu, Y.-Y. Wu, X.-M. Zhang, R.-C. Sun, Fabrication and characterization of regenerated cellulose films using different ionic liquids, *J. Spectrosc.* 2014 (2014) 1–8.
- F. Hoelkeskamp, Process for production of cuprammonium cellulose articles, US patent 3110546 A, 1963.
- T. Welton, Room-temperature ionic liquids. Solvents for synthesis and catalysis, *Chem. Rev.* 99 (1999) 2071–2084.
- S. Mallakpour, M. Dinari, Ionic liquid as green solvents: progress and prospects, in: A. Mohammad Inamuddin (Ed.), *Green Solvents II. Properties and Applications of Ionic Liquids*, Springer, Dordrecht, 2012, p. 506.
- K.M. Gupta, J. Jiang, Cellulose dissolution and regeneration in ionic liquids: a computational perspective, *Chem. Eng. Sci.* 121 (2015) 180–189.
- J. Wang, J. Luo, S. Feng, H. Li, Y. Wan, X. Zhang, Recent development of ionic liquid membranes, *Green. Energy Environ.* 1 (2016) 43–61.
- M. Ottaway, Use of thermogravimetry for proximate analysis of coals and cokes, *Fuel* 61 (1982) 713–716.
- D. Ferreira, R. Magalhães, P. Taveira, A. Mendes, Effective adsorption equilibrium isotherms and breakthroughs of water vapor and carbon dioxide on different adsorbents, *Ind. Eng. Chem. Res.* 50 (2011) 10201–10210.
- J.C. Santos, F.D. Magalhães, A. Mendes, Contamination of zeolites used in oxygen production by PSA: effects of water and carbon dioxide, *Ind. Eng. Chem. Res.* 47 (2008) 6197–6203.
- L.M. Robeson, Correlation of separation factor versus permeability for polymeric membranes, *J. Membr. Sci.* 62 (1991) 165–185.
- S.C. Rodrigues, M. Andrade, F.D. Magalhães, A. Mendes, Carbon membranes with extremely high separation performance and stability, unpublished results.
- M. Sevilla, A.B. Fuertes, The production of carbon materials by hydrothermal carbonization of cellulose, *Carbon* 47 (2009) 2281–2289.

- [59] C.S.R. Freire, A.J.D. Silvestre, C.P. Neto, M.N. Belgacem, A. Gandini, Controlled heterogeneous modification of cellulose fibers with fatty acids: effect of reaction conditions on the extent of esterification and fiber properties, *J. Appl. Polym. Sci.* 100 (2006) 1093–1102.
- [60] Y.-J. Fu, K.-S. Liao, C.-C. Hu, K.-R. Lee, J.-Y. Lai, Development and characterization of micropores in carbon molecular sieve membrane for gas separation, *Microporous Mesoporous Mater.* 143 (2011) 78–86.
- [61] C. Araujo-Andrade, F. Ruiz, J.R. Martínez-Mendoza, H. Terrones, Infrared and Raman spectra, conformational stability, ab initio calculations of structure, and vibrational assignment of α and β glucose, *J. Mol. Struct.: THEOCHEM* 714 (2005) 143–146.
- [62] J. Ibarra, E. Muñoz, R. Moliner, FTIR study of the evolution of coal structure during the coalification process, *Org. Geochem.* 24 (1996) 725–735.
- [63] D. Giolacu, F. Ciocacu, V.I. Popa, Amorphous cellulose - structure and characterization, *Cellul. Chem. Technol.* 45 (2011) 13–21.
- [64] J.M. Chalmers, P.R. Griffiths (Eds.), *Handbook of Vibrational Spectroscopy*, John Wiley & Sons, Chichester, 2002.
- [65] B.M. Kabyemela, T. Adschiri, R.M. Malaluan, K. Arai, Glucose and fructose decomposition in subcritical and supercritical water: detailed reaction pathway, mechanisms and kinetics, *Ind. Eng. Chem. Res.* 38 (1999) 2888–2895.
- [66] A.C. Lua, T. Yang, Effect of activation temperature on the textural and chemical properties of potassium hydroxide activated carbon prepared from pistachio-nut shell, *J. Colloid Interface Sci.* 274 (2004) 594–601.
- [67] N.D. Hutson, R.T. Yang, Theoretical basis for the Dubinin-Radushkevitch (D-R) adsorption isotherm equation, *Adsorption* 3 (1997) 189–195.
- [68] D. Cazorla-Amorós, J. Alcañiz-Monge, M.A. de la Casa-Lillo, A. Linares-Solano, CO_2 as an adsorptive to characterize carbon molecular sieves and activated carbons, *Langmuir* 14 (1998) 4589–4596.
- [69] S. Lagorsse, F.D. Magalhães, A. Mendes, Carbon molecular sieve membranes: sorption, kinetic and structural characterization, *J. Membr. Sci.* 241 (2004) 275–287.
- [70] M. Teixeira, M. Campo, D.A. Tanaka, M.A. Tanco, C. Magen, A. Mendes, Carbon- Al_2O_3 -Ag composite molecular sieve membranes for gas separation, *Chem. Eng. Res. Des.* 90 (2012) 2338–2345.
- [71] S. Nguyen, D.D. Do, K. Haraya, K. Wang, The structural characterization of carbon molecular sieve membrane (CMSM) via gas adsorption, *J. Membr. Sci.* 220 (2003) 177–182.
- [72] C. Nguyen, D.D. Do, Adsorption of supercritical gases in porous media: determination of micropore size distribution, *J. Phys. Chem. B* 103 (1999) 6900–6908.
- [73] S. Fu, E.S. Sanders, S. Kulkarni, Y.-H. Chu, G.B. Wenz, W.J. Koros, The significance of entropic selectivity in carbon molecular sieve membranes derived from 6FDA/DETDA:DABA(3:2) polyimide, *J. Membr. Sci.* 539 (2017) 329–343.
- [74] M. Rungta, L. Xu, W.J. Koros, Structure–performance characterization for carbon molecular sieve membranes using molecular scale gas probes, *Carbon* 85 (2015) 429–442.
- [75] H. Suda, K. Haraya, Gas permeation through micropores of carbon molecular sieve membranes derived from kapton polyimide, *J. Phys. Chem. B* 101 (1997) 3988–3994.
- [76] J. Koresch, A. Soffer, Study of molecular sieve carbons. Part 1.-Pore structure, gradual pore opening and mechanism of molecular sieving, *J. Chem. Soc., Faraday Trans. 1* (76) (1980) 2457–2471.
- [77] X. He, J.A. Lie, E. Sheridan, M.-B. Hägg, Preparation and characterization of hollow fiber carbon membranes from cellulose acetate precursors, *Ind. Eng. Chem. Res.* 50 (2011) 2080–2087.
- [78] J.A. Lie, M.-B. Hägg, Carbon membranes from cellulose and metal loaded cellulose, *Carbon* 43 (2005) 2600–2607.
- [79] S. Lagorsse, F.D. Magalhães, A. Mendes, Aging study of carbon molecular sieve membranes, *J. Membr. Sci.* 310 (2008) 494–502.